



ELSEVIER

Contents lists available at ScienceDirect

## Biosensors and Bioelectronics

journal homepage: [www.elsevier.com/locate/bios](http://www.elsevier.com/locate/bios)

# Microscale loop-mediated isothermal amplification of viral DNA with real-time monitoring on solution-gated graphene FET microchip



Dawoon Han, Rohit Chand, Yong-Sang Kim\*

School of Electronic and Electrical Engineering, Sungkyunkwan University, Suwon, Gyeonggi 16419, South Korea

## ARTICLE INFO

## Article history:

Received 17 June 2016

Received in revised form

29 August 2016

Accepted 31 August 2016

Available online 4 September 2016

## Keywords:

Viral DNA

LAMP

Graphene

FET

Real-time

Microchip

## ABSTRACT

Rapid and reliable molecular analysis of DNA for disease diagnosis is highly sought-after. FET-based sensors fulfill the demands of future point-of-care devices due to its sensitive charge sensing and possibility of integration with electronic instruments. However, most of the FETs are unstable in aqueous conditions, less sensitive and requires conventional Ag/AgCl electrode for gating. In this work, we propose a solution-gated graphene FET (SG-FET) for real-time monitoring of microscale loop-mediated isothermal amplification of DNA. The SG-FET was fabricated effortlessly with graphene as an active layer, on-chip co-planar electrodes, and polydimethylsiloxane-based microfluidic reservoir. A linear response of about 0.23 V/pH was seen when the buffers from pH 5–9 were analyzed on the SG-FET. To evaluate the performance of SG-FET, we monitored the amplification of Lambda phage gene as a proof-of-concept. During amplification, protons are released, which gradually alters the Dirac point voltage ( $V_{\text{Dirac}}$ ) of SG-FET. The resulting device was highly sensitive with a femto-level limit of detection. The SG-FET could easily produce a positive signal within 16.5 min of amplification. An amplification of 10 ng/ $\mu\text{l}$  DNA for 1 h produced a  $\Delta V_{\text{Dirac}}$  of 0.27 V. The sensor was tested within a range of  $2 \times 10^2$  copies/ $\mu\text{l}$  (10 fg/ $\mu\text{l}$ ) to  $2 \times 10^8$  copies/ $\mu\text{l}$  (10 ng/ $\mu\text{l}$ ) of target DNA. Development of this sensing technology could significantly lower the time, cost, and complications of DNA detection.

© 2016 Elsevier B.V. All rights reserved.

## 1. Introduction

Even with the tremendous development in bio-sensing technologies, the diagnosis of viral diseases still follows enzyme-linked immunosorbent assay (ELISA) and blotting based analysis. These conventional methods to detect biomarkers require a high-cost labeling process and have a complex detection sequence with long analysis time. Thus, a much of valuable time is lost in diagnosis rather than for the treatment. Likewise, most of the reported biosensors require an additional reporter molecule and intricate sensor components. Therefore, rapid, simple, and accurate diagnostic devices are needed to diagnose the disease efficiently before its advancement.

Recently, loop-mediated isothermal amplification (LAMP) is gaining attention for its outstanding amplification and rapid diagnostic ability (Notomi et al., 2000; Parida et al., 2004; Shirato et al., 2007; Thai et al., 2004). LAMP is a gene amplification technique that uses a *Bst* DNA polymerase and multiple primers to amplify the template DNA in the isothermal condition and in a short time with high selectivity. In earlier days, monitoring of

LAMP relied on optical methods, due to the change in turbidity by the released magnesium pyrophosphate precipitate as a byproduct during amplification (Mori et al., 2004). Lately, a number of miniaturized LAMP sensors with electrical analysis of amplicon have been reported. The single temperature condition for the gene amplification during LAMP is advantageous for developing a point-of-care (POC) system (Hsieh et al., 2012; Sayad et al., 2016; Sun et al., 2015; Veigas et al., 2014).

Graphene, a single carbon layer of graphite structure, has also emerged as a material of interest for fabricating biosensors. It has a large surface area, high electrical conductivity, excellent mechanical strength, and can be functionalized easily. Its outstanding properties and biocompatibility have influenced applications in numerous biosensors (He et al., 2012; Lv et al., 2010; Reiner-Rozman et al., 2015). Among various kinds of graphene-based sensors, a solution-gated field effect transistor (SG-FET), in which the gate and graphene active layer are separated by electrolyte instead of the dielectric insulator is a promising sensing platform. SG-FET is a better biosensor because it works on the electrical field based high transconductance (Hess et al., 2011). SG-FET based biosensors have proved to be highly sensitive, selective, and stable. The electrons in carbons of graphene active layer are all exposed outside the plane, which makes it very sensitive to subtle changes such as a change in pH or DNA attachment (Dong et al., 2010; Ohno et al., 2009; Yan

\* Corresponding author.

E-mail address: [yongsang@skku.edu](mailto:yongsang@skku.edu) (Y.-S. Kim).

et al., 2014; Zhang et al., 2014). The other major FET and pH based sensing platform is ion-sensitive FET (IS-FET) and was first reported 40 years ago. Bergveld et al. have extensively discussed the advancement of IS-FETs as sensors (Bergveld, 2003). Generally, IS-FETs are fabricated on a silicon substrate using CMOS process (Huang et al., 2015; Moser et al., 2016). Although IS-FETs have proven their worth, it is laborious to fabricate silicon and CMOS processed IS-FETs. Consequently, with silicon as a substrate, flexible IS-FET sensors are quite not possible. The usual structures of IS-FET and SG-FET embody a gate (reference) electrode immersed in the electrolyte from outside. This external electrode hinders the miniaturization of the device for portable use. Additionally, an internal fluid network is essential for creating a multiplexed lab-on-a-chip.

Several groups have attempted electrical detection of DNA amplification, in the past. Most of these reports achieved success in terms of DNA detection, but the presented techniques are expensive and complex to implement. Pourmand et al. reported a charge perturbation based detection of DNA synthesis. However, it requires immobilization of DNA on gold, which is tedious (Pourmand et al., 2006). Similarly, an electrochemical-based study of LAMP suggested conversion of the released pyrophosphate into electrochemically active molybdophosphate (Xie et al., 2015). However, a real-time monitoring of amplification is not possible following this study. Additionally, numerous other works on DNA detection through hybridization or covalent bonding on graphene transistors have been done (Chen et al., 2013; Dong et al., 2010; Green and Norton, 2015; Guo et al., 2011; Yin et al., 2012), but the real-time monitoring of DNA amplification on solution-gated graphene transistor has seldom been attempted.

Therefore, in this work, a monolithic solution-gated graphene FET is presented for the real-time monitoring of LAMP of viral DNA. The FET was fabricated on a glass substrate containing thin-film coplanar electrodes instead of silicon substrate and conventional Ag/AgCl electrode. The label-free sensing of DNA was depended on the change in Dirac point voltage ( $V_{\text{Dirac}}$ ) of FET, due to the release of protons during LAMP (Toumazou et al., 2013). We demonstrate the potential of SG-FET to quantify Lambda phage gene in real-time. Development of this sensing technology could

significantly lower the time, cost, and complications of DNA detection in the future.

## 2. Experimental

### 2.1. Fabrication of solution-gated graphene FET

The overall scheme for graphene transfer, microchannel fabrication, and SG-FET fabrication is shown in Fig. S1. We fabricated two FETs with common gate electrode on one substrate for multiplexed analysis; however, in this study, each FET was independently used (Fig. 1(a) and (b)). Coplanar gold electrodes for source, drain, and gate were patterned through standard photolithography and thermal evaporator on a glass substrate (Han et al., 2013). In summary, the AZ-1512 photoresist was spin-coated on glass and patterned using UV-exposure. After patterning, titanium (supporting layer) followed by gold was deposited on the glass in a vacuum thermal evaporator. The additional photoresist was removed by ultra-sonicating the glass in an acetone bath. The width of the patterned electrodes was 1 mm with a separation of 1 mm between each of them. The gate electrode exposed inside the fluid channel provided gate voltage through the electrolyte.

Graphene layer grown by chemical vapor deposition was purchased from Graphenea (Spain). The copper (Cu) foil containing graphene layer was cut in the size of  $3 \times 3$  mm. A thin layer of polydimethylsiloxane (PDMS) (sylgard 184, Dow Corning, USA, A: B=9:1) was spin coated on the graphene/Cu sheet and cured in a dry oven for 30 min, at 75 °C. After curing, the PDMS/graphene/Cu sheet was floated on  $\text{FeCl}_3$  (0.25 mg/ml) solution for 30 min, at room temperature to etch the Cu. After Cu etching, the transparent PDMS/graphene sheet was washed with copious amount of DI water. The cleaned PDMS/graphene was later placed on glass substrate containing patterned gold electrodes. The PDMS/graphene sheet was aligned on the source and drain electrode under an optical microscope. The graphene sheet was allowed to bond with the glass substrate by incubating at 75 °C for 3 min. Finally, the PDMS thin film was removed from the graphene using tweezers. A negatively molded PDMS-based microfluidic channel was

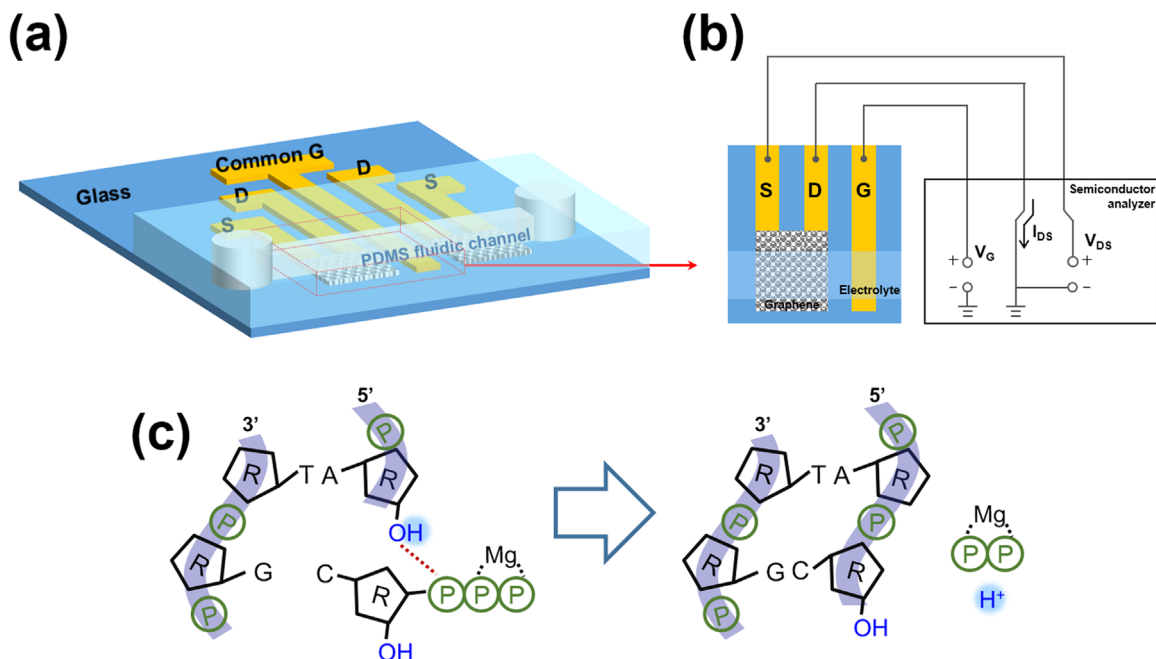


**Fig. 1. Solution-gated graphene FET (SG-FET):** (a) schematic of SG-FET couple with common gate; where S, D, and G are source, drain, and gate electrodes respectively, (b) measurement setup of a single SG-FET, and (c) mechanism of proton release during DNA synthesis.

bonded on the graphene FET after UV-ozone treatment (Han et al., 2013). The fluid channel had a width and height of 1000 and 120  $\mu\text{m}$ , respectively. Therefore, the active area of graphene was  $3 \times 1 \text{ mm}^2$ . The thus fabricated SG-FET was used for the real-time monitoring of viral DNA amplification.

## 2.2. pH sensing using SG-FET

To verify the pH sensing ability of SG-FET, 2 mM Tris-HCl buffers with pH ranging from 5 to 9 were used. The Tris-HCl buffer was injected using a syringe into the fluid channel of SG-FET and electrical response of the SG-FET was measured for each pH (Fig. 1 (a)). The electrical analysis on SG-FET was performed using an HP 4145B semiconductor analyzer (Fig. 1(b)). The pH of the buffers and LAMP products was measured by a thin rod type pH electrode (HI 1083B, HANNA Ins.).

## 2.3. Loop-mediated isothermal amplification of viral DNA

The viral DNA (Lambda phage genomic DNA, 0.3  $\mu\text{g}/\mu\text{l}$ ) used in this study was obtained from Bio Basic Inc. (Korea). The phage DNA was serially diluted with 10 mM Tris-HCl (pH 7.8) in the range from  $2 \times 10^2$  copies/ $\mu\text{l}$  (10 fg/ $\mu\text{l}$ ) to  $2 \times 10^8$  copies/ $\mu\text{l}$  (10 ng/ $\mu\text{l}$ ). At first, 25  $\mu\text{l}$  LAMP reaction mixture composed of 0.5X Thermopol<sup>®</sup> buffer (New England Biolabs, M0275S), forward inner primer (1.6  $\mu\text{M}$ , FIP), backward inner primer (1.6  $\mu\text{M}$ , BIP), forward outer primer (0.2  $\mu\text{M}$ , F3), backward outer primer (0.2  $\mu\text{M}$ , B3), *Bst* DNA polymerase (8 U, New England Biolabs, M0275S), dNTPs (1.4 mM), betaine (0.8 M, Sigma-Aldrich),  $\text{MgSO}_4$  (8 mM), and DNA (1  $\mu\text{l}$ ) was prepared. The sequences of the primers for LAMP were as follows (Mori et al., 2004):

5'-AGGCCAAGCTGCTTGCGGTAGCCGGACGCTACCAGCTTCT-3' (FIP),  
 5'-AAAACCTCAAATCAACAGCGC-3' (F3),  
 5'-CAGGACGCTGTGGCATTGCAGATCATAGTAAAGCGCCACGC-3' (BIP),  
 5'-GACGGATATCACCAGCATCA-3' (B3).

5  $\mu\text{l}$  of the above reaction the mixture was injected using a syringe in the microchannel and the inlets and outlets were filled with mineral oil to prevent the evaporation of reaction mixture. The LAMP was conducted at 65  $^\circ\text{C}$  in a conventional thermocycler (C1000<sup>™</sup>, BIORAD) and as well as in the SG-FET microfluidic chip. The heat for the on-chip amplification was supplied using a thermal hot chuck (MS tech, MST-1000B). Finally, the LAMP products were analyzed by the gel-doc system in 2% agarose gel. The real-time monitoring of LAMP on SG-FET was performed by measuring the I-V curve at intervals of 5 min.

## 3. Result and discussion

### 3.1. Characterization of transferred graphene sheet

In this work, a modified polymer supported etching transfer method was used to transfer graphene on the SG-FET (Kang et al., 2012). The commonly used poly(methyl methacrylate) (PMMA) for transferring graphene leaves its traces even after soaking in hot acetone. The PMMA residues after acetone cleaning have been causing problems such as doping effects (Shin et al., 2012). Therefore, we replaced the PMMA to PDMS, as it does not need any liquid mediated elimination step (You and Pak, 2014). The characterization of graphene sheet transferred using PDMS on the SG-FET was performed by measuring the intensity ratio of Raman spectra at 532 nm wavelength (Fig. S2). The D peak represents the defects in graphene, while the ratio of G and 2D peaks represents the number of the graphene sheet. A high-sharp 2D-peak and low

G-peak were observed at 2676 and 1592  $\text{cm}^{-1}$  respectively, which signifies that the transferred graphene is a pure monolayer sheet (Ferrari et al., 2006).

### 3.2. Characterization of solution-gated graphene FET

The schematic of the fabricated SG-FET is shown in Fig. 1(a) and (b). As can be seen, the thin-film source, drain, and gate electrodes were fabricated in the same plane on a glass substrate. This facilitated the attachment of PDMS microchannel on the SG-FET, and overall a monolithic biosensor. The source and drain electrodes were insulated from the gate electrode using the PDMS microfluidic channel. To prevent the leakage current between source and gate electrode, the microchannel ensured that only the graphene active layer and gate electrode is exposed to the electrolyte. The length and width of the exposed graphene active layer were 1 and 3 mm, respectively.

When the gate voltage is applied at SG-FET, two electrical double layers (EDL), which are regarded as a capacitor is formed at the interface of gate-electrolyte and electrolyte-graphene. The overall capacitance of interface is composed of fixed Helmholtz layers (HDLs) and Gouy-Chapman diffuse double layers (GC DLs), so the total capacitance C can be described as Eq. (1) (Palazzo et al., 2015):

$$C = \left( \frac{1}{C_{HDL}} + \frac{1}{C_{GC DL}} \right)^{-1} \quad (1)$$

The gate voltage can modulate the channel conductance of SG-FET. The representative performance of SG-FET is presented by transfer curve, which is the channel current ( $I_{DS}$ ) between source and drain as a function of gate voltage ( $V_G$ ) at fixed drain voltage ( $V_{DS}$ ). The transfer curve of SG-FET shows ambipolar characteristic which has both hole current of p-channel and electron current of n-channel without off current. The voltage at lowest current when Fermi level ( $E_F$ ) is modulated to the charge neutrality point is the switching point between hole current and electron current. This charge neutrality point is called as the Dirac point voltage ( $V_{Dirac}$ ) (Yan et al., 2014). The  $V_{Dirac}$  can be shifted by doping effect of adsorbed molecules. Schedin et al. observed that  $\text{NO}_2$  and  $\text{NH}_3$  act as acceptors and donors on graphene surface, respectively (Schedin et al., 2007). In case of donor induced,  $E_F$  moves toward lowest unoccupied molecular orbital (LUMO) level and in case of acceptor induced,  $E_F$  moves toward highest occupied molecular orbital (HOMO) level. The increase of charge carriers can move  $E_F$  level of graphene and result in shift of  $V_{Dirac}$ .

Moreover, total gate capacitance (tens of  $\mu\text{F cm}^{-2}$ ), which is composed of two EDL capacitors and graphene quantum capacitance, is pretty higher than typical FET with a thermal oxide gate insulator (Yan et al., 2014). This means that SG-FET can operate under less than 1 V of gate voltage, according to the channel current Eq. (2) (Chen et al., 2010):

$$I_{DS} \approx \frac{W}{L} \mu C_i |V_G - V_{Dirac}| V_{DS} \cdot \text{for } |V_G - V_{Dirac}| \gg |V_{DS}| \quad (2)$$

As can be seen in Fig. 2(a), the lower working voltage from 0 to 2 V range is good for biosensors because it can prevent the damage of biological samples from electrical power. A low operating voltage can also benefit in designing a battery-powered hand-held sensor.

### 3.3. pH sensing using SG-FET

The real-time monitoring of the LAMP on SG-FET was based on the release of protons during the amplification and thus the change in local surface pH. Therefore, at first, we analyzed the

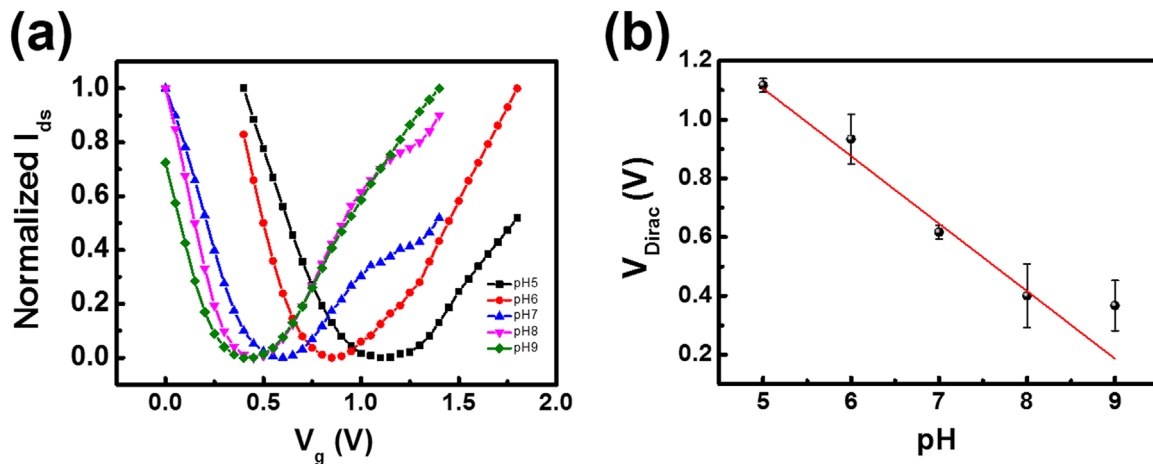


**Fig. 2.** The response of SG-FET at different pH buffers: (a) Transfer curves of SG-FET at pH 5–9, (b) Relationship between pH and  $V_{Dirac}$ . Error bar represents the standard deviation of 3 independent analysis. Buffer: 2 mM Tris–HCl.

ability of SG-FET to distinguish between buffers at different pH. The buffers were injected through the microchannel and the corresponding electrical response was measured. A response characteristic of SG-FET at different pH buffers is shown in Fig. 2. The  $V_{Dirac}$  shifted towards positive and negative when the SG-FET was exposed to acidic and basic buffer, respectively. The ionic groups present in buffer acts as a dopant and shift the  $V_{Dirac}$  of SG-FET. A good relationship was seen between the pH and change in the  $V_{Dirac}$  with an average response of 0.23 V/pH. The average rate of shift in  $V_{Dirac}$  was higher in acidic condition (0.25 V/pH) compared with the basic condition (0.125 V/pH). However, the buffers around neutral pH (6–8) produced a higher change in the  $V_{Dirac}$  due to the availability of more free reactive elements on the graphene layer. This higher sensitivity around the neutral pH is beneficial for the real-time monitoring of LAMP. Some of the previously reported graphene FET based pH sensor proposed an opposite trend where the  $V_{Dirac}$  increased along with the increase in pH (Ang et al., 2008; Ohno et al., 2009; Sohn et al., 2013). However, Lee et al. proposed that in the case of an SG-FET, the direction of  $V_{Dirac}$  shift depends on the concentration and composition of buffers as well (Lee et al., 2015). In his work, the  $V_{Dirac}$  shifted towards the positive direction in response to increasing pH, if the buffer contained a low concentration of phosphate ions. Contrarily, if the buffer contained a high concentration of phosphate ions, the  $V_{Dirac}$  shifted towards the negative with increasing pH. The type and concentration of the ionic group in the buffer decides the direction of  $V_{Dirac}$  shift. We report an average response of 0.23 V/pH, which is many folds higher than the previously reported sensitivity of 0.099 mV/pH (Ang et al., 2008), and 71 mV/pH (Ameri et al., 2016) for graphene oxide based FET and 0.0262 V/pH for CMOS ISFET (Huang et al., 2015).

#### 3.4. pH change during the LAMP

The pH-sensitive SG-FET was adopted as the LAMP based sensor for viral DNA. During DNA amplification, the hydroxyl group of nucleotide on the growing strand attacks the alpha-phosphate of deoxyribose nucleoside triphosphates (dNTP) (Fig. 1 (c)). This result in the addition of a new nucleotide to the growing DNA strand and a pyrophosphate and hydrogen ion is released as byproducts. The liberated hydrogen ion (proton) induces a change in the pH of the solution on the graphene surface. The change of pH signifies the successful amplification of DNA and was monitored using the SG-FET.

To minimize the ion charging effect on SG-FET, we first optimized the concentration of buffer used for LAMP. A low ionic

strength or concentration of buffer is important to maximize the effect of releasing protons on the SG-FET surface. For this, different sets of LAMP were carried out in buffer with concentration ranging from 0.3X to 0.8X. Fig. S3 shows the resolved LAMP amplicon in agarose gel. An attenuated amplification was observed when LAMP was performed in 0.3X and 0.4X buffers. Therefore, the LAMP was further performed in 0.5X buffer for the real-time monitoring on the SG-FET.

The gradual change in the pH during LAMP was first verified using a commercial pH meter and thin type pH electrode. A  $2 \times 10^8$  copies/ $\mu$ l of viral DNA was amplified through LAMP in a thermocycler and the change in pH was measured at intervals of 10 min for 1 h. Analysis of amplicon showed a continuous decrease in pH as the LAMP commenced, with a saturation at about 40 min (Fig. 3). The LAMP for 60 min produced a  $\Delta$ pH of 0.7. However, no considerable change in the pH was seen when no template was added in the reaction mixture (Fig. 3). This confirms that the LAMP can be monitored in real-time on SG-FET based on the change in pH.

#### 3.5. Real-time LAMP detection using SG-FET

The real-time LAMP detection using SG-FET was performed after filling the fluid channel with LAMP mixture containing target viral DNA, primers, and 0.5X reaction buffer. The amplification of viral DNA and the electrical measurement was carried out simultaneously. The electrical measurement was performed after

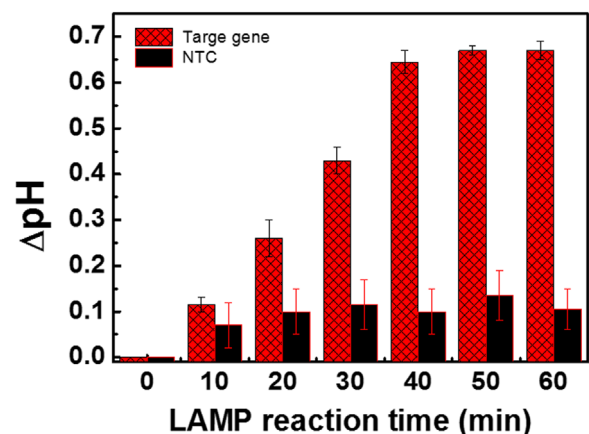


**Fig. 3.** Change of pH during LAMP in a thermocycler:  $2 \times 10^8$  (Target gene) and 0 (NTC) copies/ $\mu$ l of Lambda phage DNA.

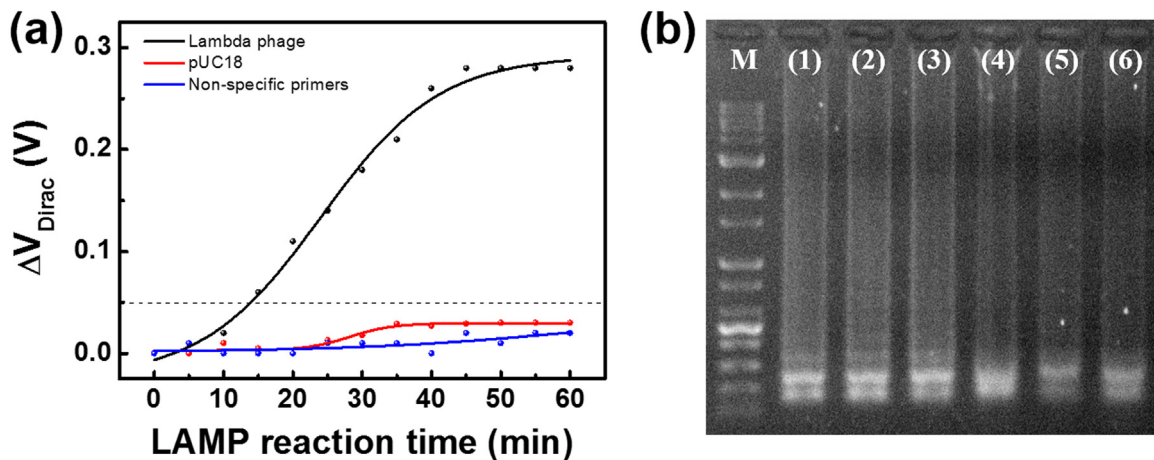


**Fig. 4.** LAMP of Lambda phage DNA: (a) Real-time response of SG-FET during on-chip LAMP of  $2 \times 10^8$  copies/ $\mu\text{l}$  of DNA (Black), pUC18 DNA as a negative control (Red), and  $2 \times 10^8$  copies/ $\mu\text{l}$  of DNA with a non-specific primer set (Blue). (b) Image of resolved amplicons in agarose gel: (M) 1.5 kb marker; (1)  $2 \times 10^8$ , (2)  $2 \times 10^7$ , (3)  $2 \times 10^6$  copies/ $\mu\text{l}$  of DNA in thermocycler; (4)  $2 \times 10^8$ , (5)  $2 \times 10^7$ , (6)  $2 \times 10^6$  copies/ $\mu\text{l}$  of DNA on SG-FET. Buffer: 0.5X Thermopol<sup>®</sup> buffer. (For interpretation of the references to color in this figure legend, the reader is referred to the web version of this article.)

every 5 min to obtain a real-time information. The progress of DNA amplification gradually decreased the pH of the mixture. The real-time shift of  $V_{\text{Dirac}}$  due to decreasing pH can be seen in Fig. 4 (a). LAMP of  $2 \times 10^8$  copies/ $\mu\text{l}$  (10 ng/ $\mu\text{l}$ ) of viral DNA for 60 min produced a 0.275 V shift in the  $V_{\text{Dirac}}$ . The SG-FET could sensitively discriminate between the target and non-target DNA amplification. We incubated the pUC18 DNA (negative control) with the primer set meant for the Lambda phage DNA. No amplification of pUC18 DNA (Fig. 4(a), red line) produced an insignificant change in the  $V_{\text{Dirac}}$  of SG-FET, thus proving the selectivity of this analysis. Similarly, the LAMP of Lambda phage DNA with a non-specific set of primer (Fig. 4(a), blue line) also produced no shift in the  $V_{\text{Dirac}}$ . Fig. 4(b) shows the resolution of LAMP products from different initial template concentrations amplified in a thermocycler and on SG-FET. The comparison of amplicons confirms the efficient working of SG-FET as a LAMP device.

To verify the ability of SG-FET as a sensitive real-time LAMP sensor, 7 different concentrations of viral DNA, ranging from  $2 \times 10^2$  copies/ $\mu\text{l}$  (10 fg/ $\mu\text{l}$ ) to  $2 \times 10^8$  copies/ $\mu\text{l}$  (10 ng/ $\mu\text{l}$ ) were amplified and analyzed. The response of SG-FET is shown in Fig. 5. The SG-FET showed a stable performance and a typical sigmoidal response curve of DNA amplification was seen, whereas the mixture with no template DNA produced no considerable change in the  $V_{\text{Dirac}}$ .

The threshold time ( $T_t$ ) was calculated from the Fig. 5 and is

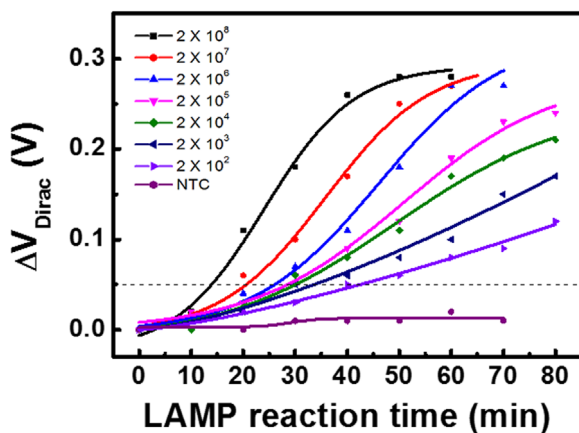


**Fig. 5.** The real-time response of SG-FET based LAMP monitoring system:  $\Delta V_{\text{Dirac}}$  after amplification of initial template DNA concentrations from 0 (NTC) to  $2 \times 10^8$  copies/ $\mu\text{l}$ . Buffer: 0.5X Thermopol<sup>®</sup> buffer.

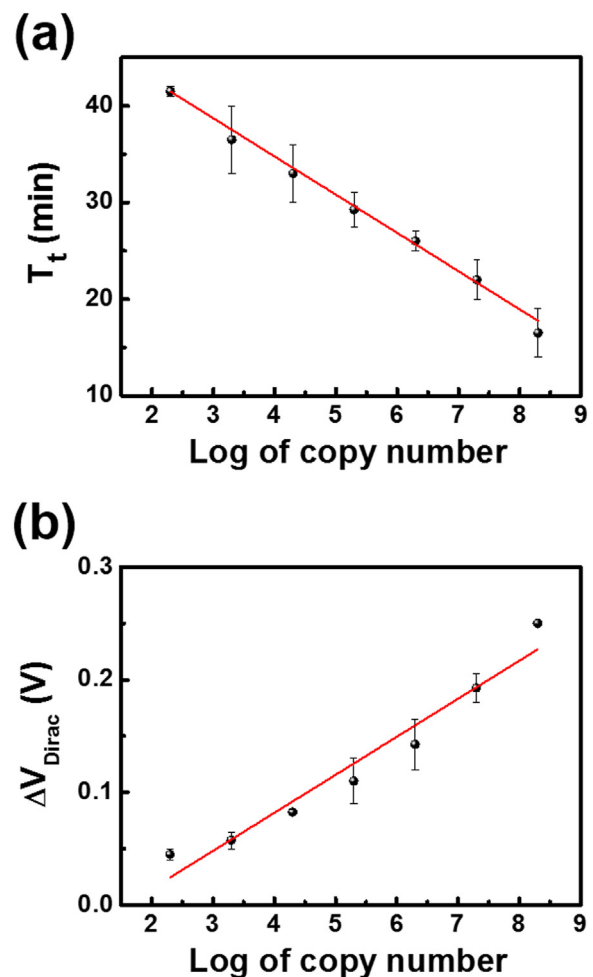


**Fig. 6.** The relationship between SG-FET response and template DNA concentration: (a) threshold time at  $\Delta V_{\text{Dirac}}$  of 0.05 V and copy number of DNA and (b)  $\Delta V_{\text{Dirac}}$  at 40 min and copy number of DNA. Error bar represents the standard deviation of 3 independent analysis.

plotted in Fig. 6(a). The reaction time that produced a  $\Delta V_{\text{Dirac}}$  of 0.05 V was considered as the threshold time. A progressive increase in the  $T_t$  ( $R^2=0.996$ ) was seen with the decreasing concentration of initial template DNA. From the Fig. 6(a), it can be

inferred that the SG-FET is highly sensitive with a minimum signal time of 16.5 min for  $2 \times 10^8$  copies/ $\mu\text{l}$ . The change in the  $V_{\text{Dirac}}$  after 40 min of amplification with respect to the initial template concentration is also summarized in Fig. 6(b). The  $\Delta V_{\text{Dirac}}$  increased with the increasing concentration of initial template DNA concentration. The device showed a limit-of-detection of  $2 \times 10^2$  copies/ $\mu\text{l}$  of viral DNA. From these results, we affirm the successful fabrication of graphene-based solution-gated FET and its application in LAMP based sensing of viral DNA.

Recently, Toumazou et al. reported an ISFET based sensor for electrically monitoring the amplification of DNA (Kalofonou and Toumazou, 2013; Purushothaman et al., 2002, 2006; Toumazou et al., 2013). The ISFET showed better performance with a  $T_t$  of 20 min for  $1 \times 10^3$  copies of DNA. In a similar work, Veigas et al. also reported a LAMP monitor based on tantalum pentoxide electrolyte-insulator-semiconductor (Veigas et al., 2014). The sensor showed a linear response for  $1 \times 10^8$ – $10^{11}$  copies of DNA with a  $T_t$  of 10 min ( $10^{11}$  copies), which is much higher than the present work. On the contrary, most of the reported graphene FET based DNA sensors only study the hybridization of DNA strands. To the best of our knowledge, this is the only work reporting SG-FET for the real-time electrical monitoring of DNA amplification. The analysis involved a label-free DNA amplification detection without the use of any dye or additional ‘reporting’ material. We could efficiently amplify and detect DNA with just a 5  $\mu\text{l}$  of the reaction mixture, which is much lower than several other reports. The direct detection of DNA amplification using graphene makes this work inexpensive and attractive for the future wearable healthcare devices.

#### 4. Conclusion

The solution-gated graphene FET comprising coplanar thin-film electrodes was developed in this work. The FET was integrated with a PDMS microchannel that works as an insulating layer and sample reservoir. Analysis of buffers from pH range 5–9 produced a linear response of 0.23 V/pH. The SG-FET was employed to monitor real-time loop-mediated isothermal amplification of DNA. The protons released during the amplification altered the  $V_{\text{Dirac}}$  of the FET. As a proof of concept, we successfully amplified and detected Lambda phage gene. The SG-FET showed a good response to the increasing initial template and amplicon concentration. Using SG-FET, we could efficiently detect the viral DNA within 16.5 min. The detection limit was observed to be  $2 \times 10^2$  copies/ $\mu\text{l}$  that corresponds to 10 fg/ $\mu\text{l}$  of DNA. The proposed SG-FET is highly sensitive, stable, low-cost, hassle-free, and can be integrated with other components for developing a lab-on-a-chip.

#### Acknowledgements

This work was funded by Korea Small and Medium Business Administration under the program ‘‘Business for Cooperative R&D between Industry, Academy, and Research Institute’’ in 2015 (grant No. C0353887).

#### Appendix A. Supplementary material

Supplementary data associated with this article can be found in the online version at <http://dx.doi.org/10.1016/j.bios.2016.08.115>.

#### References

- Ameri, S.K., Singh, P.K., Sonkusale, S.R., 2016. *Anal. Chim. Acta.*
- Ang, P.K., Chen, W., Wee, A.T.S., Loh, K.P., 2008. *J. Am. Chem. Soc.* 130 (44), 14392–14393.
- Bergveld, P., 2003. *Sens. Actuators B: Chem.* 88 (1), 1–20.
- Chen, F., Qing, Q., Xia, J., Tao, N., 2010. *Chem. Asian J.* 5 (10), 2144–2153.
- Chen, T.-Y., Loan, P.T.K., Hsu, C.-L., Lee, Y.-H., Tse-Wei Wang, J., Wei, K.-H., Lin, C.-T., Li, L.-J., 2013. *Biosens. Bioelectron.* 41, 103–109.
- Dong, X., Shi, Y., Huang, W., Chen, P., Li, L.-J., 2010. *Adv. Mater.* 22 (14), 1649–1653.
- Ferrari, A.C., Meyer, J.C., Scardaci, V., Casiraghi, C., Lazzeri, M., Mauri, F., Piscanec, S., Jiang, D., Novoselov, K.S., Roth, S., Geim, A.K., 2006. *Phys. Rev. Lett.* 97 (18), 187401.
- Green, N.S., Norton, M.L., 2015. *Anal. Chim. Acta* 853, 127–142.
- Guo, S.-R., Lin, J., Penchev, M., Yengel, E., Ghazinejad, M., Ozkan, C.S., 2011. *J. Nanosci. Nanotechnol.* 11 (6), 5258–5263.
- Han, D., Chand, R., Shin, I.-S., Kim, Y.-S., 2013. *Anal. Methods* 5 (23), 6814.
- He, Q., Wu, S., Yin, Z., Zhang, H., 2012. *Chem. Sci.* 3 (6), 1764.
- Hess, L.H., Hauf, M.V., Seifert, M., Speck, F., Seyller, T., Stutzmann, M., Sharp, I.D., Garrido, J.A., 2011. *Appl. Phys. Lett.* 99 (3), 033503.
- Hsieh, K., Patterson, A.S., Ferguson, B.S., Plaxco, K.W., Soh, H.T., 2012. *Angew. Chem. Int. Ed.* 51 (20), 4896–4900.
- Huang, X., Yu, H., Liu, X., Jiang, Y., Yan, M., Wu, D., 2015. *IEEE Trans. Biomed. Eng.* 62 (9), 2224–2233.
- Kalofonou, M., Toumazou, C., 2013. *Sens. Actuators B* 178, 572–580.
- Kang, J., Shin, D., Bae, S., Hong, B.H., 2012. *Nanoscale* 4 (18), 5527.
- Lee, M.H., Kim, B.J., Lee, K.H., Shin, I.-S., Huh, W., Cho, J.H., Kang, M.S., 2015. *Nanoscale* 7 (17), 7540–7544.
- Lv, W., Guo, M., Liang, M.-H., Jin, F.-M., Cui, L., Zhi, L., Yang, Q.-H., 2010. *J. Mater. Chem.* 20 (32), 6668.
- Mori, Y., Kitao, M., Tomita, N., Notomi, T., 2004. *J. Biochem. Biophys. Methods* 59 (2), 145–157.
- Moser, N., Lande, T., Toumazou, C., Georgiou, P., 2016. *IEEE Sens. J.* 16 (17), 6496–6514.
- Notomi, T., Okayama, H., Masubuchi, H., Yonekawa, T., Watanabe, K., Amino, N., Hase, T., 2000. *Nucl. Acids Res* 28 (12), 63e.
- Ohno, Y., Maehashi, K., Yamashiro, Y., Matsumoto, K., 2009. *Nano Lett.* 9 (9), 3318–3322.
- Palazzo, G., De Tullio, D., Magliulo, M., Mallardi, A., Intranuovo, F., Mulla, M.Y., Favia, P., Vikholm-Lundin, I., Torsi, L., 2015. *Adv. Mater.* 27 (5), 911–916.
- Parida, M., Posadas, G., Inoue, S., Hasebe, F., Morita, K., 2004. *J. Clin. Microbiol.* 42 (1), 257–263.
- Pourmand, N., Karhanek, M., Persson, H.H.J., Webb, C.D., Lee, T.H., Zahradnikova, A., Davis, R.W., 2006. *Proc. Natl. Acad. Sci.* 103 (17), 6466–6470.
- Purushothaman, S., Toumazou, C., Ou, C.-P., 2006. *Sens. Actuators B* 114 (2), 964–968.
- Purushothaman, S., Toumazou, C., Georgiou, J., 2002. *Circuits and Systems, 2002. ISCAS 2002. IEEE International Symposium on* 4, IV-169–IV-172.
- Reiner-Rozman, C., Larisika, M., Nowak, C., Knoll, W., 2015. *Biosens. Bioelectron.* 70, 21–27.
- Sayad, A.A., Ibrahim, F., Uddin, S.M., Pei, K.X., Mohktar, M.S., Madou, M., Thong, K.L., 2016. *Sens. Actuators B* 227, 600–609.
- Schedin, F., Geim, A.K., Morozov, S.V., Hill, E.W., Blake, P., Katsnelson, M.I., Novoselov, K.S., 2007. *Nat. Mater.* 6 (9), 652–655.
- Shin, D.-W., Lee, H.M., Yu, S.M., Lim, K.-S., Jung, J.H., Kim, M.-K., Kim, S.-W., Han, J.-H., Ruoff, R.S., Yoo, J.-B., 2012. *ACS Nano* 6 (9), 7781–7788.
- Shirato, K., Nishimura, H., Saijo, M., Okamoto, M., Noda, M., Tashiro, M., Taguchi, F., 2007. *J. Virol. Methods* 139 (1), 78–84.
- Sohn, I.-Y., Kim, D.-J., Jung, J.-H., Yoon, O.J., Nguyen Thanh, T., Tran Quang, T., Lee, N.-E., 2013. *Biosens. Bioelectron.* 45, 70–76.
- Sun, Y., Quyen, T.L., Hung, T.Q., Chin, W.H., Wolff, A., Bang, D.D., 2015. *Lab Chip* 15 (8), 1898–1904.
- Thai, H.T.C., Le, M.Q., Vuong, C.D., Parida, M., Minekawa, H., Notomi, T., Hasebe, F., Morita, K., 2004. *J. Clin. Microbiol.* 42 (5), 1956–1961.
- Toumazou, C., Shepherd, L.M., Reed, S.C., Chen, G.I., Patel, A., Garner, D.M., Wang, C.-J.A., Ou, C.-P., Amin-Desai, K., Athanasiou, P., Bai, H., Brizido, I.M.Q., Caldwell, B., Coomber-Alford, D., Georgiou, P., Jordan, K.S., Joyce, J.C., La Mura, M., Morley, D., Sathyavrudhan, S., Temelso, S., Thomas, R.E., Zhang, L., 2013. *Nat. Methods* 10 (7), 641–646.
- Veigas, B., Branquinho, R., Pinto, J.V., Wojcik, P.J., Martins, R., Fortunato, E., Baptista, P.V., 2014. *Biosens. Bioelectron.* 52, 50–55.
- Xie, S., Yuan, Y., Chai, Y., Yuan, R., 2015. *Anal. Chem.* 87 (20), 10268–10274.
- Yan, F., Zhang, M., Li, J., 2014. *Adv. Healthc. Mater.* 3 (3), 313–331.
- Yin, Z., He, Q., Huang, X., Zhang, J., Wu, S., Chen, P., Lu, G., Chen, P., Zhang, Q., Yan, Q., Zhang, H., 2012. *Nanoscale* 4 (1), 293–297.
- You, X., Pak, J.J., 2014. *Sens. Actuators B* 202, 1357–1365.
- Zhang, M., Liao, C., Yao, Y., Liu, Z., Gong, F., Yan, F., 2014. *Adv. Funct. Mater.* 24 (7), 978–985.